



OPEN

Enantiomers of 2-methylglutamate and 2-methylglutamine selectively impact mouse brain metabolism and behavior

Adam M. Wawro¹, Chandresh R. Gajera¹, Steven A. Baker¹, Robert K. Leśniak², Curt R. Fischer², Nay L. Saw³, Mehrdad Shamloo^{3,4} & Thomas J. Montine¹✉

Imbalance of excitatory and inhibitory neurotransmission is implicated in a wide range of psychiatric and neurologic disorders. Here we tested the hypothesis that insertion of a methyl group on the stereogenic alpha carbon of L-Glu or L-Gln would impact the γ -aminobutyric acid (GABA) shunt and the glutamate-glutamine cycle. (S)-2-methylglutamate, or (S)-2MeGlu, was efficiently transported into brain and synaptosomes where it was released by membrane depolarization in a manner equivalent to endogenous L-Glu. (R)-2MeGlu was transported less efficiently into brain and synaptosomes but was not released by membrane depolarization. Each enantiomer of 2MeGlu had limited activity across a panel of over 30 glutamate and GABA receptors. While neither enantiomer of 2MeGlu was metabolized along the GABA shunt, (S)-2MeGlu was selectively converted to (S)-2-methylglutamine, or (S)-2MeGln, which was subsequently slowly hydrolyzed back to (S)-2MeGlu in brain. rac-2MeGln was also transported into brain, with similar efficiency as (S)-2MeGlu. A battery of behavioral tests in young adult wild type mice showed safety with up to single 900 mg/kg dose of (R)-2MeGlu, (S)-2MeGlu, or rac-2MeGln, suppressed locomotor activity with single ≥ 100 mg/kg dose of (R)-2MeGlu or (S)-2MeGlu. No effect on anxiety or hippocampus-dependent learning was evident. Enantiomers of 2MeGlu and 2MeGln show promise as potential pharmacologic agents and imaging probes for cells that produce or transport L-Gln.

The amino acid L-glutamine and the neurotransmitters L-glutamate and γ -aminobutyric acid (GABA) are linked metabolically via the glutamate-glutamine cycle and the GABA shunt (Fig. 1)^{1,2}. Imbalance of the complex metabolic interplay between excitatory (mostly glutamatergic) and inhibitory (mostly GABAergic) neurotransmission has been implicated in a wide range of psychiatric and neurologic disorders. Inherited deficiencies in the glutamate-glutamine cycle, either glutamine synthetase (GS) deficiency (OMIM 610015) or glutaminase deficiency (OMIM 138280), yield neonatal-infantile epileptic encephalopathy and early death^{3,4}. Inherited deficiencies within the GABA shunt include SSADH deficiency (OMIM 271980) and GABA-transaminase deficiency (OMIM 613163) that are characterized by language and motor delay, cognitive impairment, ataxia, autistic behaviors, hallucinations, and epilepsy in both children and adults^{5,6}, with elevated γ -hydroxybutyrate (GHB) and/or GABA^{7,8}. Prevalent diseases are proposed to derive at least in part from more subtle imbalance of excitatory and inhibitory neurotransmission, including mood disorders, some forms of psychosis, epilepsy, Alzheimer's disease, and Parkinson's disease⁹. The prospect of restoring balance to these opposing systems has been the focus of many candidate therapeutics, some of which have gone on to wide-spread clinical application: receptor specific agonists, antagonists, and allosteric modulators, transporter inhibitors, gene transfer, and most recently cell therapy^{10,11}. None of these approaches target the metabolic balance of the GABA shunt or the glutamate-glutamine cycle, and as yet none has had a major impact on alleviating the common psychiatric or neurodegenerative diseases listed above. Here we tested the hypothesis that insertion of a methyl group on the stereogenic alpha carbon of L-glutamate or L-glutamine would provide novel tools to modulate the metabolic balance within the the GABA shunt or the glutamate-glutamine cycle, and perhaps have utility as molecular imaging agents or drugs that influence behavior.

¹Department of Pathology, Stanford University, Stanford, USA. ²ChEM-H, Stanford University, Stanford, USA. ³Behavioral and Functional Neuroscience Laboratory, Stanford University, Stanford, USA. ⁴Department of Neurosurgery, Stanford University, Stanford, USA. ✉email: tmontine@stanford.edu

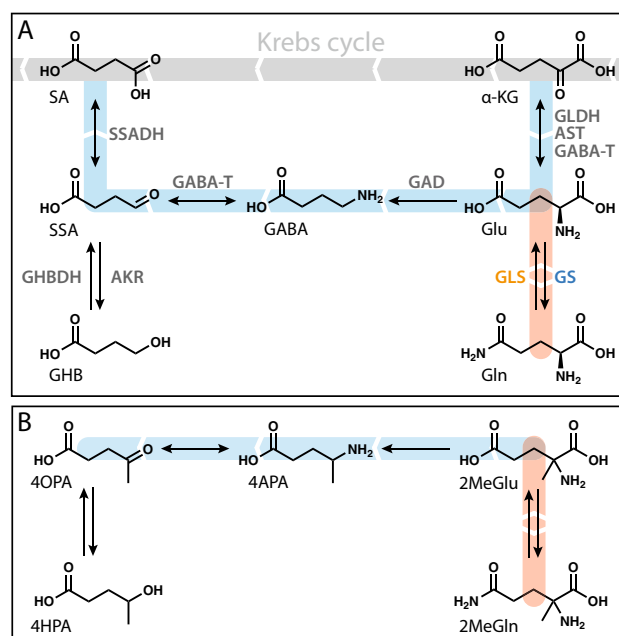


Figure 1. L-Glutamate is involved in the GABA shunt (blue arrows) off of the Krebs cycle and in the glutamate-glutamine cycle (red arrows) (A). Glutamate amidation proceeds primarily in astrocytes (blue font), while the reverse reaction scheme occurs in neurons (orange font). For simplicity the transport steps are not shown. Hypothetical metabolic scheme of 2MeGlu into methyl analogues of Glu metabolites (B). SA and α-KG have no exact analogues and are not shown in the figure. AKR aldo-keto reductase, AST aspartate transaminase, GABA-T GABA transaminase, GAD glutamate decarboxylase, GHBBDH gamma-hydroxybutyrate dehydrogenase, GLDH glutamate dehydrogenase, GLS glutaminase, GS glutamine synthetase, SSADH succinic semialdehyde dehydrogenase, GABA γ-aminobutyric acid, GHB γ-hydroxybutyric acid, Gln L-glutamine, Glu L-glutamate, α-KG α-ketoglutarate, SA succinic acid, SSA succinic semialdehyde.

In addition to 2MeGlu, we evaluated its hypothetical metabolites, i.e., analogues of the major Glu metabolites methylated at the carbon atom located at the α position in Glu; these include: 2-methylglutamine (2MeGln, the Gln analogue), 4-aminopentanoic acid (4APA, the GABA analogue), 4OPA (4-oxopentanoic acid or levulinic acid, the SSA analogue), and 4-hydroxypentanoic acid (4HPA, the GHB analogue). α-KG and SA have no corresponding methylated analogues; the presence of the hypothetical carbon atom at the α position would not be possible without breaking the existing C–C bonds. Since α-KG and SA connect Glu to the Krebs cycle, 2MeGlu cannot enter the cycle in a Glu-like manner.

Results

We used LC–MS/MS with HILIC and chiral HILIC-like chromatography to resolve all compounds of interest, including their structural isomers, present in biological matrices over a wide range of concentrations¹². Introduction of a methyl group on the α carbon drastically reduced the ability of the stationary phase to resolve enantiomers compared to natural amino acids, nevertheless we achieved baseline resolution of 2MeGlu and 4APA enantiomers without prior derivatization (Supplementary Figure S1).

Evaluation of the neurotransmitter-like properties was performed using mouse cerebral synaptosomes, a preparation of functional, mostly presynaptic, nerve terminals. Uptake of both enantiomers of 2MeGlu was temperature-dependent (Fig. 2A), although the S enantiomer (analogous to L-2MeGlu) was approximately three-fold faster than the R enantiomer (analogous to D-2MeGlu). Among the potential 2MeGlu metabolites, only rac-4APA was transported into synaptosomes, while 4OPA and 4HPA were not (Fig. 2B). We tested if 2MeGlu was in the neurotransmitter pool by subjecting preloaded synaptosomes to high potassium concentration-induced membrane depolarization. Both enantiomers of 2MeGlu were transported into synaptosomes during preloading; however, their potassium-induced release from vesicular storage was different (Fig. 2C). Synaptosomal concentration of the R enantiomer was not significantly altered by depolarization, whereas the S enantiomer was released upon depolarization in a manner very similar to endogenous Glu (Fig. 2E), as indicated by the relative difference of the substrate concentrations in the samples incubated under the low- and high-potassium conditions. When tested under identical conditions, rac-4APA exhibited high potassium concentration-dependent release (Fig. 2D) that was similar to endogenous GABA (Fig. 2E). Thus, (R)- and (S)-2MeGlu and rac-4APA were transported into synaptosomes, but only (S)-2MeGlu and at least one enantiomer of 4APA entered the neurotransmitter pool.

Initial metabolic assays also were performed in mouse cerebral synaptosomes, which are known to contain residual astrocytic components comprising <5% of total terminals by electron microscopic or flow cytometric detection (Supplementary Figure S2)^{13,14}. Synaptosomal concentration of rac-2MeGlu decreased slowly over time with an estimated half life of 21 min, and was not associated with the concurrent appearance of 4APA or any other

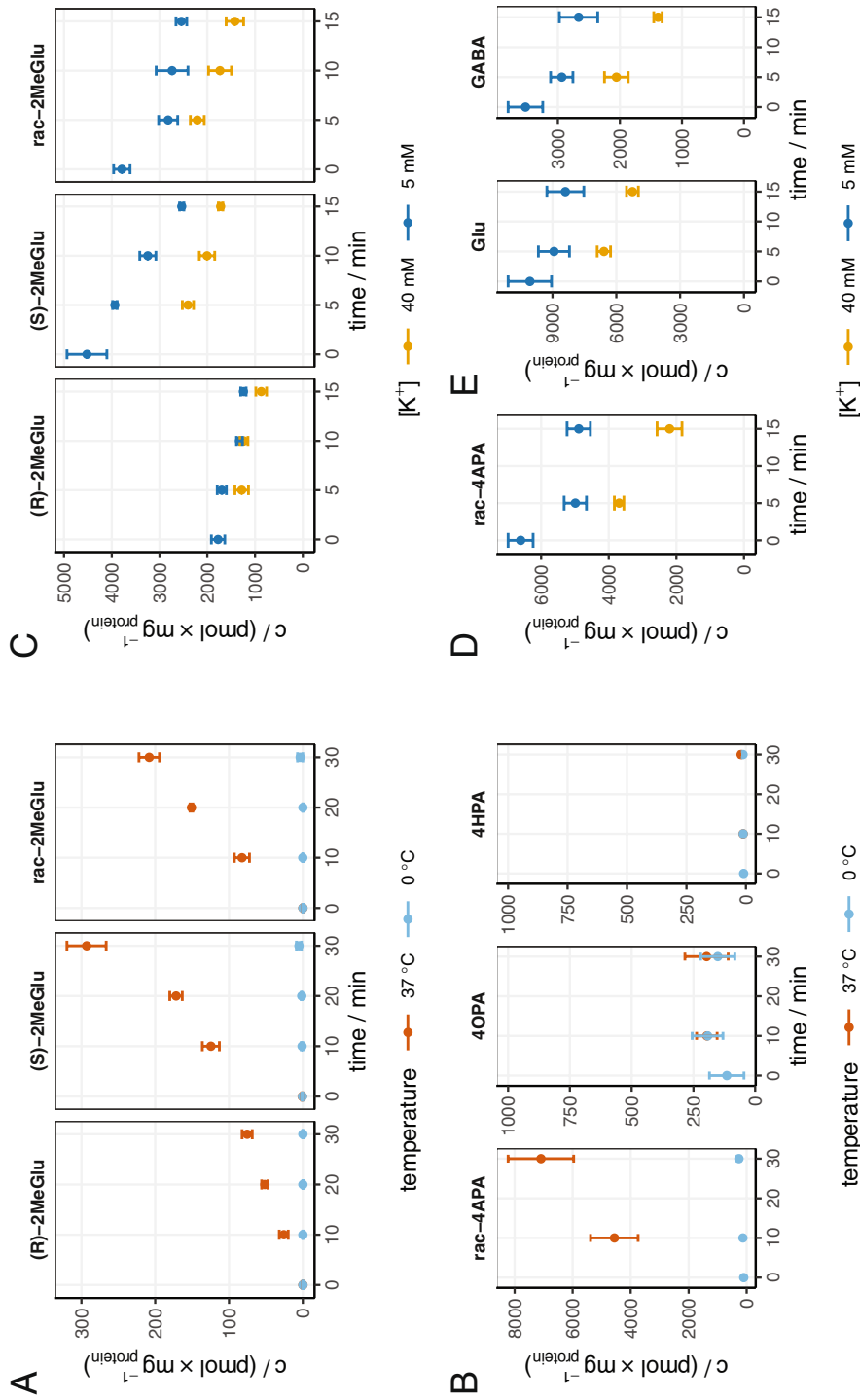


Figure 2. Synaptosomal accumulation of 2MeGlu (A) and 2Me analogues of the GABA shunt metabolic pathway (B). Synaptosomes were incubated with 10 μM substrates at 0 °C or 37 °C and the uptake was monitored over time. Error bars represent s.e.m., n = 3. Potassium-induced release of Synaptosomal 2MeGlu (C), 4APA (D) and endogenous Glu and GABA (E). Synaptosomes were preincubated with 100 μM substrate (C,D only) for 15 min at 37 °C. The pellet was washed, resuspended in normal or high-potassium KRP buffer and incubated for the times indicated at 37 °C. Data are shown as mean \pm SEM, n = 3.

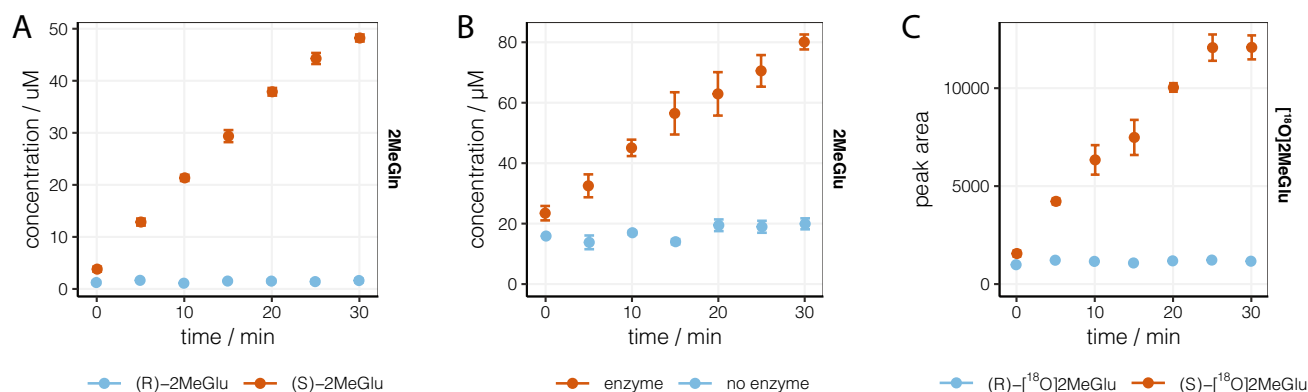


Figure 3. (A) Stereospecific conversion of 2MeGlu enantiomers by human glutamine synthetase. Reaction was performed with 10 mM substrate and 5 ng/mL enzyme in the presence of 10 mM ATP, 20 mM MgCl₂, 40 mM NH₄Cl, 25 mM 2-mercaptoethanol in 100 mM imidazole pH 7.0 buffer¹⁸. (B) Conversion of rac-2MeGln by human glutaminase GLS1. Reaction was performed with 10 mM substrate and 5 ng/mL enzyme in phosphate pH 7.4 buffer¹⁹. (C) Relative concentrations of (R)- and (S)-[¹⁸O]2MeGlu generated in the GLS1 hydrolysis assay. Data are shown as mean ± SEM, n = 3.

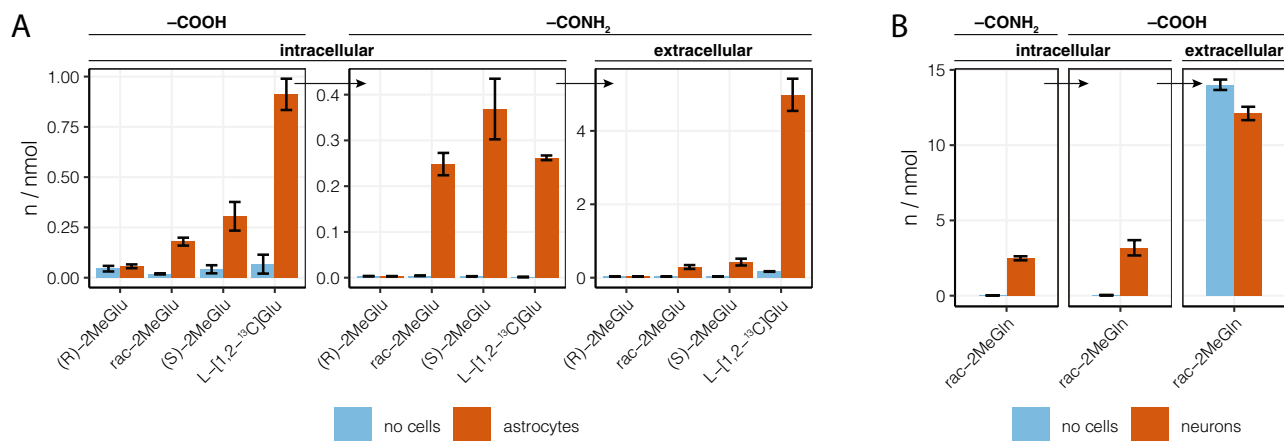


Figure 4. Cell metabolism of 2MeGlu and 2MeGln. Data are shown as mean ± SEM, n = 3. Horizontal arrows represent an uptake–conversion–release cycle. (A) Astrocyte uptake, amidation, and release of 2MeGlu and its amide derivative, 2MeGln. Total intra- and extracellular amounts of 2MeGlu or [1,2-¹³C]Glu (–COOH) and 2MeGln or [1,2-¹³C]Gln (–CONH₂) were determined in cells and media. Primary astrocyte cultures were incubated in the presence of 1 mM of racemic or enantiopure 2MeGlu or L-Glu for 2 h at 37 °C along with cell-free controls. (B) Neuronal uptake, hydrolysis, and release of 2MeGln and its hydrolyzed counterpart 2MeGlu. Total intra- and extracellular amounts of 2MeGln (–CONH₂) and 2MeGlu (–COOH) were determined in cells and media. Primary neuron cell cultures were incubated in the presence of 1 mM 2MeGln for 2 h at 37 °C along with cell-free controls.

2Me analogue within the GABA shunt, indicating that the 2Me analogues were not efficiently metabolized by this pathway's enzymes. We hypothesized that 2MeGlu might have been metabolized to 2MeGln and/or released back into the extrasynaptosomal space (Supplementary Figure S2). Indeed, rapid formation of 2MeGln along with a steady release of 2MeGlu were observed and accounted for the total concentration of all 2Me species over time, i.e., the total concentration of both 2MeGlu and 2MeGln did not change significantly over time ($P = 0.70$, repeated measures one-way ANOVA, $n = 5$) (Supplementary Figure S2), indicating that the only major metabolite of 2MeGlu in mouse synaptosomes was 2MeGln.

GS is responsible for brain metabolism of Glu to Gln. Consistent with the synaptosome results, 2MeGlu was converted by human GS to 2MeGln in the presence of ammonium ions and ATP, but the reaction was highly stereoselective towards the S enantiomer (Fig. 3A). This is another stereochemical difference with Glu, both enantiomers of which are amidated by GS¹⁵. Our results are consistent with the previous work that showed the reaction of rac-2MeGlu with GS in the presence of ATP releases 50% of inorganic phosphate obtained under identical conditions with L-Glu¹⁶. The reverse reaction was tested in vitro using human glutaminase GLS1, a phosphate-dependent amidohydrolase, which accounts for over 50% of glutaminase activity in the brain¹⁷. In order to overcome the analytical interference caused by traces of 2MeGlu present in synthetic 2MeGln, catalytic

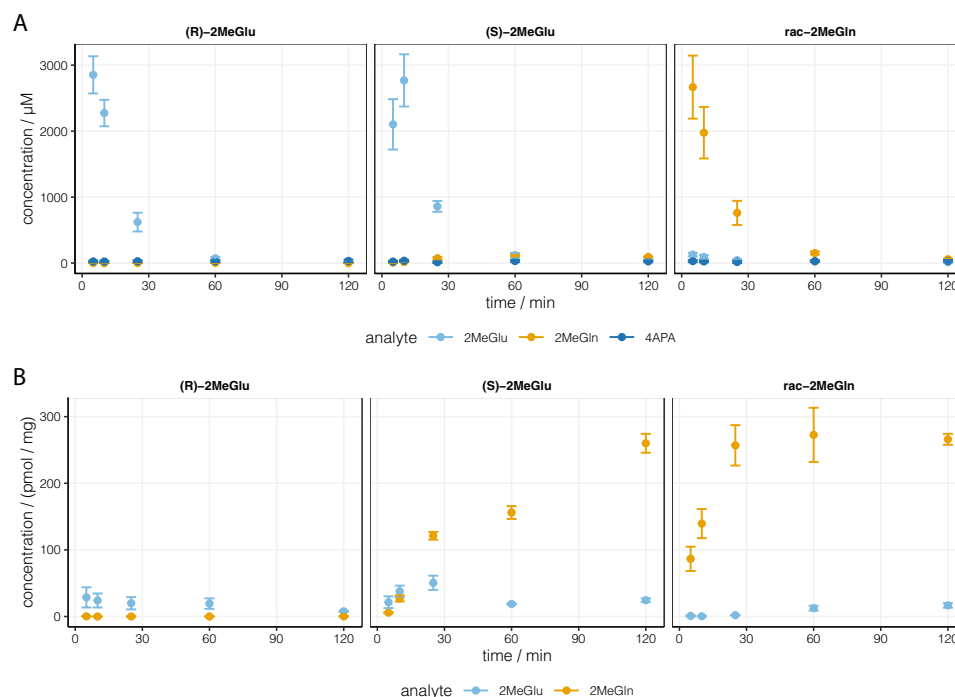


Figure 5. Pharmacokinetics of 2Me compounds and their metabolites measured in mouse serum (A) and brain (B) after IP injection of 100 mg/kg of test compounds (in columns). Concentrations are expressed per volume in the serum samples and per protein content in the brain samples. Data are shown as mean \pm SEM, $n = 3$.

hydrolysis was performed in $H_2^{18}O$ -enriched buffer. Simultaneous detection of 2MeGlu and 2MeGlu- ^{18}O allowed us to distinguish between the newly formed 2MeGlu and any preexisting impurity, and thereby quantify exclusively the former (Fig. 3B). The appearance of 2MeGlu in the samples containing rac-2MeGln indicated that at least one enantiomer of 2MeGln is a substrate for human GLS1, albeit relatively slow; the apparent reaction rate was approximately 35-fold lower compared to that of Gln ($65 \mu M/min$ vs $1.9 \mu M/min$). Chiral analysis of the isotope-labeled hydrolysis products showed that the *S* enantiomer was the exclusive product of the GLS1-catalyzed reaction (Fig. 3C).

Incubation of primary murine cerebral astrocytes with each enantiomer of 2MeGlu confirmed the stereoselective nature of 2MeGln formation observed in synaptosomes and with GS *in vitro* (Fig. 4). The *S* enantiomer was transported into astrocytes and then converted into 2MeGln. In contrast, the *R* enantiomer was not detected within astrocytes in significant amounts, and no conversion to 2MeGln was detected. Comparison with isotopically labeled L -[1,2- ^{13}C]Glu, the endogenous substrate, revealed that the intracellular concentrations of 2MeGln and [1,2- ^{13}C]Gln, made from (*S*)-2MeGlu and L -[1,2- ^{13}C]Glu respectively, were similar (0.35 nmol/well vs 0.26 nmol/well); however, the extracellular concentrations were an order of magnitude different (0.4 nmol/well vs 5.0 nmol/well), suggesting that 2MeGln was released from astrocytes at a much lower rate compared to [1,2- ^{13}C]Gln. Samples where racemic 2MeGlu was used as the substrate followed the pattern of the *S* enantiomer, although at concentrations consistently reduced 60–70%.

Enzymatic hydrolysis of 2MeGln back to 2MeGlu to complete the glutamate-glutamine cycle was tested in murine primary cerebral cortical neuron cultures (Fig. 4C). 2MeGlu was detected in the mouse neurons, although it was unclear whether it was a product of intracellular enzymatic hydrolysis of 2MeGln or direct transport from media, since traces of 2MeGlu were present in the 2MeGln synthetic product. The uptake of both enantiomers of 2MeGlu observed in synaptosomes and hydrolysis of at least one enantiomer of 2MeGln by human GLS1 suggested that both mechanisms contribute to the intracellular presence of 2MeGlu in neuron cultures. An identical experiment was performed in primary cerebral cortical neuron cultures with isotopically labeled L -[1,2- ^{13}C]Gln for comparison (data not shown). Intracellular [1,2- ^{13}C]Gln was twofold lower than 2MeGln in corresponding samples, while [1,2- ^{13}C]Glu was over fivefold lower than 2MeGlu in cells. Together with the presence of extracellular [1,2- ^{13}C]Glu, these results suggest that [1,2- ^{13}C]Gln is enzymatically hydrolyzed and transported out of the cell at a higher rate than 2MeGln.

In summary, the above *in vitro*, synaptosome, and primary cell culture experiments show that 2MeGlu and 2MeGln are transported in and out of neurons and astrocytes, similar to their non-methylated endogenous analogues, while having more restricted, stereochemically-dependent, metabolic pathways. (*S*)-2MeGlu and (*S*)-2MeGln were shown to be substrates of GS and GLS1, respectively, while their *R* enantiomers were not. In addition, the relatively low rate of extracellular release of endogenously synthesized 2MeGln suggests partial trapping of the amidation product in primary astrocytes where it was generated.

Receptor name	Receptor type	Assay type	(R)-2MeGlu	(S)-2MeGlu
GluN2A	Ionotropic	Functional	↓	–
GluN2B	Ionotropic	Functional	–	–
GluN2C	Ionotropic	Functional	–	–
GluN2D	Ionotropic	Functional	–	–
GluA2	Ionotropic	Functional	–	–
mGluR1	Metabotropic	Binding	–	–
mGluR2	Metabotropic	Binding	–	–
mGluR5	Metabotropic	Binding	–	–
NMDA nonspecific	Ionotropic	Binding	–	–
AMPA nonspecific	Ionotropic	Binding	–	–
kainate nonspecific	Ionotropic	Binding	–	–
GABA _A α1β1γ2	Ionotropic	Functional	–	–
GABA _A α1β2γ2	Ionotropic	Functional	–	–
GABA _A α1β3γ2	Ionotropic	Functional	–	–
GABA _A α2β1γ2	Ionotropic	Functional	–	–
GABA _A α2β2γ2	Ionotropic	Functional	–	–
GABA _A α2β3γ2	Ionotropic	Functional	–	–
GABA _A α3β1γ2	Ionotropic	Functional	–	–
GABA _A α3β2γ2	Ionotropic	Functional	–	–
GABA _A α3β3γ2	Ionotropic	Functional	–	–
GABA _A α4β1γ2	Ionotropic	Functional	–	–
GABA _A α4β2γ2	Ionotropic	Functional	–	–
GABA _A α4β3γ2	Ionotropic	Functional	–	–
GABA _A α4β3δ	Ionotropic	Functional	–	–
GABA _A α5β1γ2	Ionotropic	Functional	–	–
GABA _A α5β2γ2	Ionotropic	Functional	–	–
GABA _A α5β3γ2	Ionotropic	Functional	–	–
GABA _A α6β1γ2	Ionotropic	Functional	–	–
GABA _A α6β2γ2	Ionotropic	Functional	–	–
GABA _A α6β3γ2	Ionotropic	Functional	–	–
GABA _B (B1/B2)	Metabotropic	Binding	–	–
GABA _B (B1a/B2)	Metabotropic	Binding	–	–
GABA _B (B1b/B2)	Metabotropic	Binding	–	–
GABA _B (B1/B2)	Metabotropic	Functional	–	–

Table 1. Summary of glutamate and GABA receptor interaction assays. ‘↑’ or ‘↓’ arrows indicate agonist or antagonist activity, respectively. The number of arrows indicates IC₅₀/EC₅₀ in the range of 10–100 μM (one arrow), 1–10 μM (two arrows), or < 1 μM (three arrows). Interactions with EC₅₀ or IC₅₀ above 100 μM are marked as “–”.

Since GS is important to proliferation of some cancer cells²⁰, we determined the impact of both 2MeGlu enantiomers and rac-2MeGln on proliferation of glutamine-dependent MDA-MB-231 and SK-OV-3, and glutamine-independent MCF-7^{21,22}. Cell viability assays were conducted by BPS Bioscience and showed that none of the test compounds effectively inhibited cell proliferation (IC₅₀ > 100 μM) in any of the three cell lines (Supplementary Figure S3). These results aligned with our GLS1 inhibition assay, where none of the compounds displayed significant inhibitory activity (IC₅₀ > 1 mM) (Supplementary Figure S3).

We next examined pharmacokinetics of 2Me compounds in mouse blood and brain (Fig. 5). All compounds reached their maximum serum concentration within 15 min of intraperitoneal (IP) administration and were practically cleared from blood within 60 min (Fig. 5A). All tested compounds entered the brain where their kinetic profiles differed substantially (Fig. 5B). (R)-2MeGlu brain concentration peaked within 5 min at 30 pmol/mg protein and decreased over time with an estimated half life of approximately 70 min. (S)-2MeGlu reached its maximum brain concentration of 50 pmol/mg protein after 25 min, while being actively converted into its only known metabolite, 2MeGln, which concentration rose monotonically to over 250 pmol/mg protein at 120 min. Thus, (S)-2MeGlu and its metabolite (S)-2MeGln accumulated in the brain as much as tenfold more than (R)-2MeGlu. Administered rac-2MeGln yielded peak brain concentration of 2MeGln more rapidly (25 min) than injection with (S)-2MeGlu, and then was relatively constant to 120 min. Interestingly, the concentrations of 2MeGln in mouse brain at the last time point (120 min) were almost identical whether administered (S)-2MeGlu or rac-2MeGln, indicating that (S)-2MeGlu is efficiently metabolized to 2MeGln in mouse brain and could act as a prodrug/precursor. A common feature observed for both (S)-2MeGlu and rac-2MeGln is the appearance of 2MeGlu at the 60 min and 120 min time points. Previously presented results from GLS1 enzymatic assay

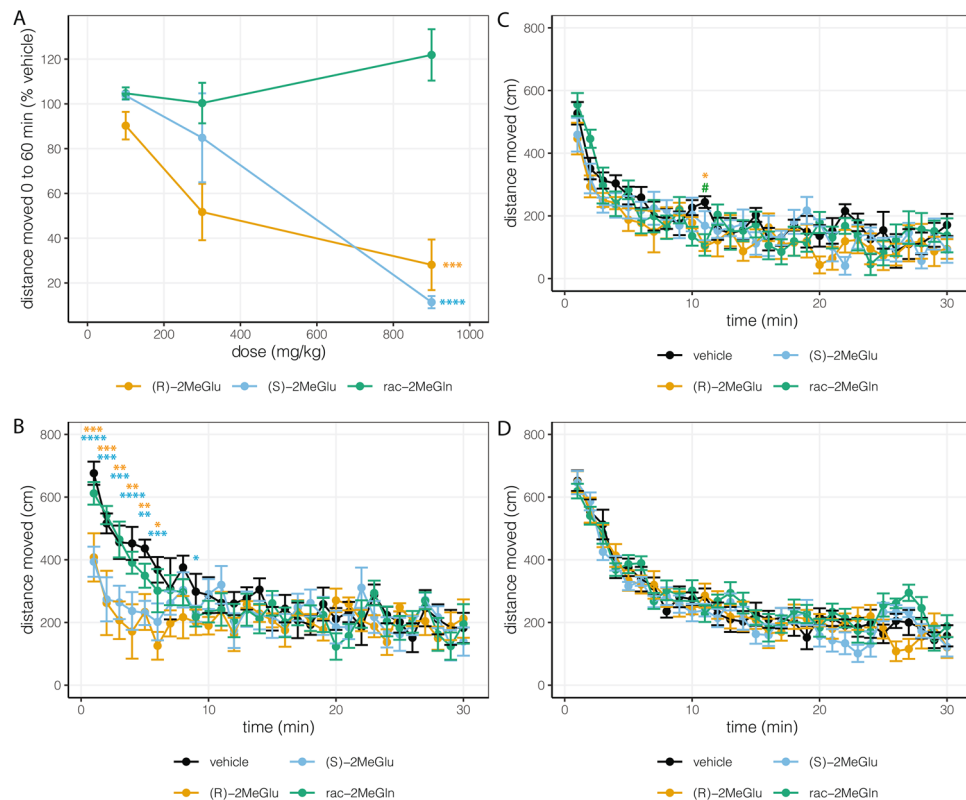


Figure 6. Exploratory and locomotor behavior in 2 month-old male C57Bl/6 mice was assessed by total distance moved in the novel cage test (A) or in the activity chamber (B–D). Mice were either injected and then immediately tested (acute groups in A–C), or injected daily for one week prior to testing (chronic groups in D). Data are shown as mean \pm SEM. (A) Dose–response for each of the three compounds vs. total distance moved from 0 to 60 min in the novel cage test expressed as % of vehicle exposed mice ($n = 3$ mice per group). Two-way ANOVA had $F_{\text{Interaction}}(4, 18) = 9.068$, $P = 0.0003$; $F_{\text{Dose}}(2, 18) = 14.91$, $P = 0.0002$; and $F_{\text{Compound}}(2, 18) = 21.89$, $P < 0.0001$. Tukey’s multiple comparison test was significantly different for rac-2MeGln vs. (R)-2MeGlu (**** $P < 0.0001$) and vs. (S)-2MeGlu (*** $P = 0.0002$). (B) Time course of activity chamber distance moved following acute 100 mg/kg had two-way repeated measures ANOVA with $F_{\text{Interaction}}(87, 580) = 1.879$, $P < 0.0001$; $F_{\text{Time}}(29, 580) = 11.44$, $P < 0.0001$; and $F_{\text{Exposure}}(3, 20) = 2.906$, $P = 0.0600$ ($n = 6$ mice per group). Dunnett’s multiple comparisons test had multiple early time points that were significantly different between vehicle and (R)-2MeGlu or between vehicle and (S)-2MeGlu (* $P < 0.05$, ** $P < 0.01$, *** $P < 0.001$, **** $P < 0.0001$); vehicle was not significantly different from rac-2MeGln at any time point. (C) Time course of activity chamber distance moved following acute 30 mg/kg had two-way repeated measures ANOVA with $F_{\text{Interaction}}(87, 580) = 0.9328$, $P = 0.6493$; $F_{\text{Time}}(29, 580) = 20.13$, $P < 0.0001$; and $F_{\text{Exposure}}(3, 20) = 1.805$, $P = 0.1786$ ($n = 6$ mice per group). Dunnett’s multiple comparisons test had one time point that was significantly different between vehicle and (R)-2MeGlu (* $P < 0.05$) or between vehicle and rac-2MeGln ($\#P < 0.05$); vehicle was not significantly different from (S)-2MeGlu at any time point. (D) Time course of activity chamber distance moved following chronic 10 mg/kg per day for one week had two-way repeated measures ANOVA with $F_{\text{Interaction}}(87, 986) = 1.22$, $P = 0.0912$; $F_{\text{Time}}(29, 986) = 62.35$, $P < 0.0001$; and $F_{\text{Exposure}}(3, 34) = 1.122$, $P = 0.3536$; ($n = 6$ mice per group). One vehicle group mouse and one (S)-2MeGlu group mouse were outliers using the ROUT method; they were removed from analysis.

suggested that (S)-2MeGln undergoes slow enzymatic hydrolysis to (S)-2MeGlu. The pharmacokinetic experiment in mice aligns with that observation; the delayed appearance of 2MeGlu in the brain after the administered compounds have been cleared from blood indicates that 2MeGlu is slowly metabolized from the 2MeGln accumulated in brain, whether the original source was rac-2MeGln or (S)-2MeGlu. Finally, brain levels of endogenous Glu, Gln, or GABA also were determined as part of these experiments; two-way ANOVA showed that endogenous brain levels of Glu, GABA, or Gln were not significantly altered by either any of the three compounds administered at 100 mg/kg or the time after compound administration from 5 to 120 min (not shown).

We then explored the pharmacodynamics of enantiopure glutamate-mimicking compounds against a broad panel of glutamate and GABA receptors in both binding and functional assays (summarized in Table 1 and detailed in Supplementary Tables S1 to S5). We deliberately assayed 2MeGlu enantiomers for activity against both glutamate and GABA receptors in case of receptor class switching as occurs with α -methyl dopamine^{23,24}. Both compounds had weak to no significant activity against the large number of glutamate and GABA receptors

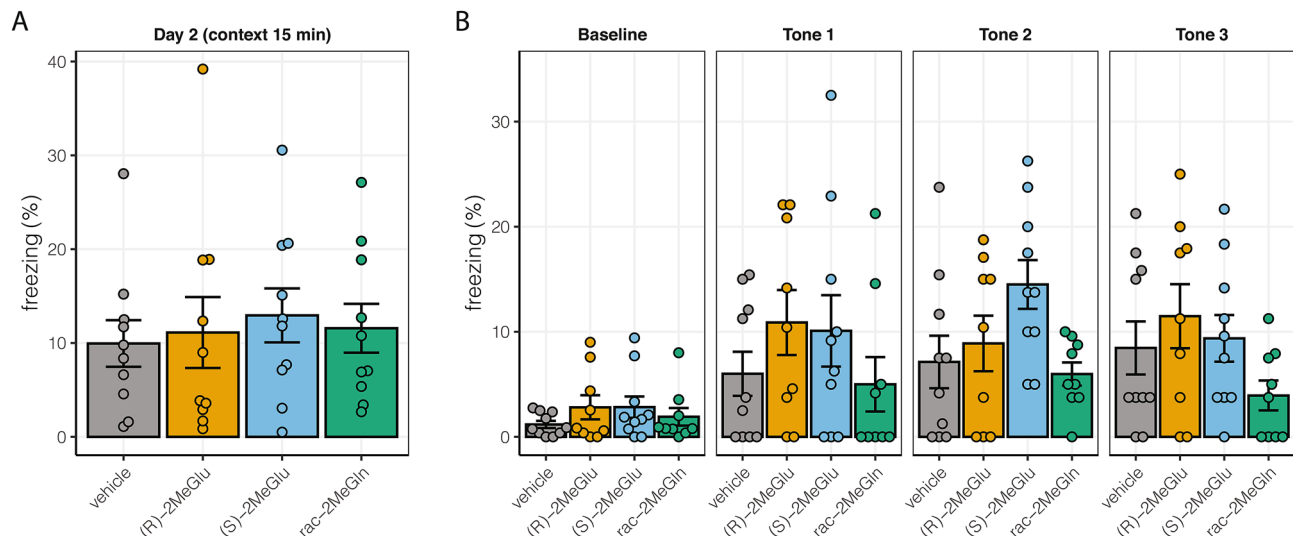


Figure 7. Behavioral effects of chronic 10 mg/kg/day IP dosing in 2 month-old male C57Bl/6 mice in fear conditioning tests on the fourth week of chronic exposure. **(A)** Freezing by the treatment group on Day 2 during contextual memory testing over 15 min. Data was not normally distributed. Kruskal–Wallis test had P approximately 0.7819. **(B)** Freezing at baseline and during each tone presentation on Day 3. Two-way repeated measures ANOVA had $F_{\text{Interaction}}(9, 102) = 1.313, P = 0.24$; $F_{\text{Tone}}(3, 102) = 13.95, P < 0.0001$; and $F_{\text{Exposure}}(3, 34) = 2.015, P = 0.13$. All bars represent mean \pm SEM, $n = 10$ mice per group.

screened. Interestingly, (S)-2MeGlu did not interact significantly with any of the tested receptors. (R)-2MeGlu exhibited weak antagonist behavior against GluN2A, one of four isoforms of the glutamate-binding subunit of *N*-methyl-D-aspartate (NMDA) receptors.

Our data suggested that 2MeGlu was a false neurotransmitter that also interfered with the glutamate-glutamine cycle. Investigators at the Stanford Behavioral and Functional Neuroscience Laboratory (SBFNL), who were blinded to the identity of the compounds being tested, performed a broad-based screen of safety and tolerability followed by tests of learning and memory, similar to the behavioral screen of transgenic mice with glutaminase deficiency¹⁷. Male 2 month-old healthy mice were injected with a single dose (100, 300, or 900 mg/kg IP) of (R)-2MeGlu, (S)-2MeGlu, or rac-2MeGln and then immediately assessed by novel cage observation and for survival. Only one mouse died 10 days after 900 mg/kg of (R)-2MeGlu. Distance moved in the novel cage was significantly decreased for both (R)-2MeGlu and (S)-2MeGlu ($P < 0.001$ for each, $n = 3$) in a dose- and time-dependent manner, indicating marked reduction in response to novelty/locomotor activity while remaining alert and responsive (Fig. 6A and Supplementary Figure S4). Next, we performed a behavioral test battery called SHIRPA (measures 23 sensorimotor functions and well being), activity chamber open field assessment, and then withdrawal from hot plate using new groups of male 2 month-old mice following a single injection of 100 or 30 mg/kg IP of one of the three compounds or vehicle ($n = 6$ per group). At the 100 mg/kg IP dose, there was no mortality, difference in latency to withdraw from hotplate, or difference on any SHIRPA score except locomotor activity for (R)-2MeGlu or (S)-2MeGlu (not shown). Distance moved in the activity chamber was significantly reduced for (R)-2MeGlu or (S)-2MeGlu compared to vehicle at all time points up to 6 min post injection with no significant difference in distance moved beyond 9 min; rac-2MeGln was not significantly different from vehicle at any time point (Fig. 6B). We repeated the acute exposure experiment in a separate set of mice now using 30 mg/kg or vehicle IP and observed modest but significant reduction in distance moved only at 11 min post injection with (R)-2MeGlu and rac-2MeGln (Fig. 6C); no significant differences on SHIRPA scores, or latency to withdraw from hot plate, were observed in the 30 mg/kg IP dose groups (not shown).

Subsequently, still-blinded experiments at SBFNL pursued behavioral impact of chronic low dose (S)-2MeGlu, (R)-2MeGlu, or rac-2MeGln in drug naïve, male, 2 month-old C57Bl/6 mice dosed with 10 mg/kg/day or vehicle IP for a month. Behavioral tests ($n = 10$ mice per group) were performed starting one week after chronic dosing and followed well established protocols: activity chamber and elevated plus maze (week 1 of testing), Y maze (week 2 of testing), Morris water maze (weeks 2 and 3 of testing), and fear conditioning (week 4 of testing)^{25–30}. There was no mortality and no significant effect of treatment on body weight over the month, distance moved in the activity chamber (Fig. 6D), time spent in the open arms in the elevated plus maze (Supplementary Figure S5), spontaneous alternation in the Y maze (Supplementary Figure S6), or learning in the Morris water maze (Supplementary Figure S7). In the fear conditioning paradigm, all treatment groups showed equivalent learning of the tone-shock association on Day 1 (Supplementary Figure S8). There was no significant effect of treatments compared to the vehicle treated group in contextual recall on Day 2 (Fig. 7A), indicating comparable hippocampal memory recall among experimental groups, consistent with the Morris water maze results. Finally, there were no significant differences detected in freezing during the cued recall or tone presentation on Day 3 between drugs and vehicle treated groups (Fig. 7B, Supplementary Figure S9).

Discussion

Methylation of the alpha carbon of neurotransmitter precursors has been used with L-dihydroxyphenylalanine (L-DOPA) to create Aldomet or α -methyl dopa, one of the first and still used antihypertensives³¹, and with L-tryptophan to create a serotonergic PET imaging agent^{32,33}. Racemic 2MeGlu is generally synthesized from levulinic acid^{34–36} and has been used in enzymatic studies^{37–41}; as a potential effector of glutamate receptors^{42–46}, transporters^{47–51}, and brain tumor cell growth⁵²; in tissue slices as a potential effector of dopamine release⁵³, ammonia balance⁵⁴, calcium uptake⁵⁵, and metabotropic receptors⁵⁶; and in animals to moderate induced circling behavior⁵⁷. Enantiomers of 2MeGlu have been obtained by separation of racemate by a variety of methods^{16,58–60}, and (S)-2MeGlu^{61–63} or (R)-2MeGlu⁶⁴ have been synthesized by a variety of approaches. (S)-2MeGlu has been tested as an inhibitor of EAAT1/2 transporters^{65,66}. As far as we are aware, despite the use of rac-2MeGlu as a congener in these experiments, mostly published from the 1950s to 1980s, no one has investigated the metabolic impact of enantiomers of 2MeGlu or 2MeGln in brain, or explored their potential enantiomer-specific activity in animals. Here, we tested the hypothesis that enantiomers of 2MeGlu or 2MeGln selectively modulate metabolism in the GABA shunt or glutamate–glutamine cycle, and may act as potentially useful pharmacologic or imaging agents.

By design, 2-MeGlu was not a substrate for GAD or GLDH and therefore progressed neither through the GABA shunt nor underwent oxidative deamination. The S enantiomer (L isomer by the convention used for natural amino acids) was avidly transported into synaptosomes and stored and released like L-Glu. While substituting for L-Glu in the neurotransmitter pool, (S)-2MeGlu did not have significant activity across a broad spectrum of glutamate and GABA receptors. In aggregate, these data support classifying (S)-2MeGlu as a false neurotransmitter. We demonstrated that only (S)-2MeGlu is a substrate for GS and thereby can enter the glutamate–glutamine cycle; however, (S)-2MeGlu was not an efficient substrate for the reverse reaction. The net effect in vivo was that the false neurotransmitter, (S)-2MeGlu, rapidly accumulated as (S)-2MeGln in brain, which was then slowly converted back to (S)-2MeGlu. Exposure to rac-2MeGln led to comparable but more rapid appearance of 2MeGln in brain, accompanied by slow generation of 2MeGlu over time. These properties lead us to propose that (S)-2MeGlu or 2MeGln might have useful applications as pharmacologic agents that alter the excitatory/inhibitory balance in brain, and perhaps as imaging agents for GS expressing or Gln transporting cells.

(R)-2MeGlu, as expected, also was not a substrate for GAD and did not progress in the GABA shunt. (R)-2MeGlu, although transported into synaptosomes, did not enter the neurotransmitter pool, suggesting that (R)-2MeGlu is a substrate for neuronal membrane transport but not synaptic vesicle transport. (R)-2MeGlu did have some weak activity at the GluN2A subunit of NMDA receptors. (R)-2MeGlu also was transported into mouse brain, but much less efficiently than the S enantiomer. (R)-2MeGlu was not a substrate for GS and so did not enter the glutamate–glutamine cycle. The net effect was that (R)-2MeGlu accesses the brain and synaptic, but not vesicular, compartments where it is isolated from the usual metabolism of L-Glu, L-Gln, or GABA, and has some weak activity at glutamate receptors.

The enantiomer-specific biochemical and metabolic properties of 2MeGlu or 2MeGln suggest that they may have useful applications as molecular imaging agents for GS expressing or Gln transporting cells, and perhaps as pharmacologic agents that could alter excitatory/inhibitory balance. We therefore pursued safety and behavioral testing in young adult, healthy, male mice. Acute, high doses of (S)-2MeGlu, (R)-2MeGlu, or rac-2MeGln had minimal mortality, and (R)-2MeGlu or (S)-2MeGlu caused temporary, marked reduction in response to novelty/locomotor activity while remaining alert and responsive to ambient noise and gentle touch. We speculate that this impressive, acute effect on mouse behavior observed at 100 mg/kg IP and higher doses may be due to temporary disturbance in glutamatergic neurotransmission from the inability of both enantiomers of 2MeGlu to be metabolized by GAD. The usefulness of such impaired response to novelty/locomotor activity is not clear but possibly could have utility in the management of patients undergoing procedures or imaging sessions. More work is needed to understand the impact of high dose on 2MeGlu enantiomers on neurotransmitter systems.

There are some limitations to our initial behavioral testing of enantiomers of 2MeGlu and 2MeGln. Although chronic, low dose exposure to compounds did not have a significant impact on behavioral tests, cumulative dosing varied over the month of exposure with our screening protocol. Future research is needed to determine more exact dose–response relationships in male mice and extend our experiments to include female mice, more detailed evaluation of impact on response to novelty vs. locomotor activity, and the effectiveness of these compounds in older mice and in models of neurological and psychiatric disorders proposed to derive in part from imbalance of excitatory and inhibitory neurotransmission.

Methods

Materials. (R)-2-methylglutamic acid, (S)-2-methylglutamic acid and rac-2-methylglutamine were made to order by Concept Life Sciences (Cheshire, UK) from racemate.

Buffer S (isotonic buffered sucrose solution): 0.32 M sucrose, 1 mM EDTA, 5 mM Tris–HCl pH 7.4. Buffer KRP (normal Krebs–Ringer phosphate buffer): 118.0 mM NaCl, 4.65 mM KCl, 1.23 mM CaCl₂, 1.18 mM KH₂PO₄, 3.54 mM MgSO₄, 15.64 mM Na₂HPO₄, 10 mM glucose. Buffer K-KRP (high-potassium Krebs–Ringer phosphate buffer): 84.3 mM NaCl, 40.5 mM KCl, 1.23 mM CaCl₂, 1.18 mM KH₂PO₄, 3.54 mM MgSO₄, 15.64 mM Na₂HPO₄, 10 mM glucose.

Synaptosome preparation. Mouse cerebral synaptosomes were prepared according to published methods¹⁴. See Supplementary Methods for details. 500 μ L aliquots of the synaptosome suspension were transferred to pre-chilled microcentrifuge tubes for experiments. Centrifugations were at 8000g for 4 min at 4 °C, unless stated otherwise, and all samples were stored at –80 °C.

Synaptosomal neurotransmitter uptake assay. To each tube, 5 μL of a test compound solution (final concentration 10 μM) in Buffer KRP or Buffer KRP alone were added. Samples were incubated at 4 $^{\circ}\text{C}$ or 37 $^{\circ}\text{C}$ for 1, 10, or 30 min and then immediately centrifuged and washed twice by resuspension–centrifugation with Buffer S (0.5 mL). Resulting pellets were resuspended in 170 μL of 0.1% aqueous formic acid and mixed with 330 μL of ACN.

Potassium-induced neurotransmitter release assay. To each tube, 2.5 μL of a test compound solution (final concentration 100 μM) in Buffer KRP or Buffer KRP alone were added. Samples were incubated for 15 min at 37 $^{\circ}\text{C}$, briefly chilled on ice, and then immediately centrifuged and washed twice with Buffer KRP. The resulting pellets were then resuspended in either Buffer KRP (500 μL) or Buffer K-KRP (500 μL). Samples were immediately centrifuged or incubated for 5, 10 or 15 min at 37 $^{\circ}\text{C}$, then centrifuged and washed with Buffer KRP. Resulting pellets were resuspended in 400 μL of 60% ACN containing 2.5 μM Glu-d5 and 2.5 μM Gln-d5 as internal standards.

Metabolism in the GABA shunt pathway in synaptosomes. To each tube, a 5 μL aliquot of a test compound solution (final concentration 100 μM) in Buffer KRP or Buffer KRP alone were added. The samples were incubated for 15 min at 37 $^{\circ}\text{C}$, briefly chilled on ice, and then immediately centrifuged and washed twice by resuspension–centrifugation with Buffer S (0.5 mL).

The pellets were then resuspended in Buffer KRP (500 μL). Samples were then immediately centrifuged or incubated for 5, 10, 15, 20, 25 or 30 min at 37 $^{\circ}\text{C}$ and then centrifuged and washed by resuspension–centrifugation with Buffer S (0.5 mL). Resulting pellets were resuspended in 170 μL of 0.1% aqueous formic acid, mixed with 330 μL of ACN.

Metabolism in the glutamate-glutamine cycle in synaptosomes. To each tube, 5 μL of 2MeGlu solution (final concentration 100 μM) in Buffer KRP or Buffer KRP alone were added. The samples were incubated for 15 min at 37 $^{\circ}\text{C}$, briefly chilled on ice, and then immediately centrifuged and washed twice by resuspension–centrifugation with Buffer S (0.5 mL). The pellets were then resuspended in Buffer KRP (200 μL). Samples were then kept on ice or incubated for 10, 20, 30, 40 or 50 min at 37 $^{\circ}\text{C}$ and then chilled on ice. Then all samples were centrifuged, 200 μL of supernatants were collected, and the pellets were suspended in 200 μL of 80% ACN. Supernatants and pellet suspensions were diluted with 250 μL of ACN and 50 μL of 10 μM d5-Glu in water as internal standard.

Catalysis of 2MeGlu C5-amidation by human glutamine synthetase. The procedure was adapted from an existing protocol¹⁸. To a reaction mixture in a 1.5 mL microcentrifuge tube containing 10 mM substrate, 10 mM ATP, 20 mM MgCl_2 , 40 mM NH_4Cl , 25 mM 2-mercaptoethanol in 100 mM imidazole–HCl buffer pH 7.0, recombinant human glutamine synthetase (final concentration: 5 ng/mL) was added. The tubes were incubated in a preheated thermomixer at 37 $^{\circ}\text{C}$ and shaken at 600 rpm (30 s on, 30 s off). 5 μL aliquots were collected in triplicate every 5 min and immediately diluted with 195 μL of cold 60% ACN containing 10 μM Glu-d5 and Gln-d5 as internal standards in a 96 well plate. After collecting all samples, 200 μL of ACN was added to all wells and the plate was shaken at 1000 rpm for 5 min at room temperature, and then stored at -80°C until analysis.

Catalysis of 2MeGln hydrolysis by GLS1 glutaminase. The procedure was adapted from an existing protocol¹⁹. To a reaction mixture in a 1.5 mL microcentrifuge tube containing 10 mM rac-2MeGln or L-Gln-¹³C2 in 100 mM phosphate pH 7.4 buffer made in 20% atom ¹⁸O water, recombinant GLS1 (final concentration: 5 ng/mL) was added. The tubes were incubated in a preheated thermomixer at 37 $^{\circ}\text{C}$ and periodically shaken at 600 rpm (30 s on, 30 s off). 5 μL aliquots were collected in triplicate every 5 min and immediately diluted with 195 μL of cold 60% ACN containing 10 μM Glu-d5 and Gln-d5 as internal standards in a 96 well plate. After collecting all samples, the plate was shaken at 1000 rpm for 5 min at room temperature, and then stored at -80°C . Before analysis the plate was thawed and 10 μL aliquots of the extracted reaction mixtures were diluted with 190 μL of 90% acetonitrile.

The quantification of the newly formed 2MeGlu in the presence of the preexisting trace amounts was performed in the following way. Peak area ratio of Glu-¹³C2 to Glu-¹³C2¹⁸O was calculated in all samples containing Glu-¹³C2. The mean ratio value was then applied to calculate the hypothetical peak area of the newly formed 2MeGlu based on the directly measured 2MeGlu-¹⁸O peak area. The ratio of the newly formed 2MeGlu peak area and the total 2MeGlu peak area was applied to calculate the concentration of the newly formed 2MeGlu from the total 2MeGlu concentration determined directly using the calibration curve.

Astrocyte transport and metabolism of 2MeGlu. Primary astrocytes from C57Bl/6 mouse brain were cultured in complete astrocyte growth medium at 37 $^{\circ}\text{C}$ at 5% CO_2 on 96 well plates. Cells were exposed to 1 mM compound in 100 μL medium for 2 h at 37 $^{\circ}\text{C}$. Supernatants were collected, centrifuged at 2500g for 10 min at 4 $^{\circ}\text{C}$. 10 μL aliquots were diluted with 190 μL 60% ACN containing 10 μM Glu-d5 and Gln-d5. Cells were quickly washed with 250 μL cold PBS twice and suspended in 200 μL of 60% ACN containing 10 μM Glu-d5 and Gln-d5. All samples were shaken at 1000 rpm for 5 min and then stored at -80°C .

Neuronal transport and metabolism of 2MeGln. The procedure was adapted from an existing protocol⁶⁷. Wild-type (WT) C57Bl/6J mating pairs were housed according to Stanford IACUC protocol. On day P0, pups were euthanized and brains dissected in cold HBSS (without Ca^{2+} or Mg^{2+}). The forebrain was micro-

dissected to isolate the cortex and hippocampus. These brain regions were minced in cold HBSS before trypsinization at 37 °C for 9 min, followed by trituration, through 2 glass polished Pasteur pipettes. The resulting cell suspension was passed through a 100 µm filter to isolate single cells which were sedimented at 250g for 5 min. The cell pellet was then resuspended in complete Neural Basal Media (Neural Basal Media + Glutamax + B-27 Plus Supplement + Pen/Strep) + 10%FBS, counted using a hemocytometer and plated at 1×10^6 cells per mL into a 24 well plate (1 mL per well) coated with poly-D-lysine and laminin. Cultures were grown at 37 °C/5% CO₂ in a tissue culture incubator. Media was exchanged 50% on day 1 in vitro (1DIV) with fresh complete Neural Basal Media without FBS and thereafter every other day with the same media. On 3DIV the media was spiked with 2 µM AraC to limit glial growth. On 10DIV the media was completely replaced with 500 µL Neural Basal Media containing B-27 Plus Supplement + Pen/Strep without added Glutamax but instead containing 1 mM substrate at 37 °C for 2 h. The supernatants were collected, centrifuged at 16,000g for 5 min at 4 °C. 10 µL aliquots were diluted with 190 µL 60% ACN containing 5 µM Glu-d5 and Gln-d5. The cells were washed with 500 µL PBS twice and suspended in 200 µL of 60% ACN containing 5 µM Glu-d5 and Gln-d5. All samples were shaken at 800 rpm for 5 min and then stored at -80 °C until analysis.

In vivo animal studies. Behavioral tests were performed on 2 month-old, male, C57Bl/6 mice. We selected male mice because SBFNL historical controls are male mice. First, we assessed safety and tolerability of acute exposure to our novel chemicals through the following sequence of tests immediately following IP injection: maximum tolerated dose with novel cage observation at 100, 300, or 900 mg/kg, and then SHIRPA, activity chamber, and then hot plate latency using 100 or 30 mg/kg IP in different drug naïve mice. Second, we investigated the impact of chronic exposure to 10 mg/kg (3-times lower dose than that with minimal acute impact on locomotor activity) daily IP injection starting one week prior to assessment of locomotion in the activity chamber and elevated plus maze (week 1), or learning and memory with Y maze (week 2), Morris water maze (weeks 2 and 3), and then fear conditioning (week 4) according to established protocols^{25–30}, including not counterbalancing the escape platform location^{68,69}. Animals were dosed daily from 3 to 5 PM after the conclusion of each behavioral testing session. While the time from first dose for each behavioral test is different, our experimental protocol allows for efficient testing of chronic effects of novel compounds. See Supplementary Methods for details.

Approval for animal experiments. All procedures followed the National Institute of Health guidelines and were approved by the Stanford University's Administrative Panel on Laboratory Animal Care.

Data availability

Data generated during this study are available from the corresponding author on reasonable request.

Received: 16 October 2020; Accepted: 31 March 2021

Published online: 14 April 2021

References

- Bak, L. K., Schousboe, A. & Waagepetersen, H. S. The glutamate/GABA-glutamine cycle: Aspects of transport, neurotransmitter homeostasis and ammonia transfer. *J. Neurochem.* **98**, 641–653 (2006).
- Bouché, N. & Fromm, H. GABA in plants: Just a metabolite?. *Trends Plant Sci.* **9**, 110–115 (2004).
- Rumping, L. *et al.* Identification of a loss-of-function mutation in the context of glutaminase deficiency and neonatal epileptic encephalopathy. *JAMA Neurol.* **76**, 342–350 (2019).
- Häberle, J. *et al.* Congenital glutamine deficiency with glutamine synthetase mutations. *N. Engl. J. Med.* **353**, 1926–1933 (2005).
- Pearl, P. L. *et al.* Clinical spectrum of succinic semialdehyde dehydrogenase deficiency. *Neurology* **60**, 1413–1417 (2003).
- Lapalme-Remis, S. *et al.* Natural history of succinic semialdehyde dehydrogenase deficiency through adulthood. *Neurology* **85**, 861–865 (2015).
- Jakobs, C. *et al.* Urinary excretion of gamma-hydroxybutyric acid in a patient with neurological abnormalities. The probability of a new inborn error of metabolism. *Clin. Chim. Acta* **111**, 169–178 (1981).
- Chambliss, K. L. *et al.* Two exon-skipping mutations as the molecular basis of succinic semialdehyde dehydrogenase deficiency (4-hydroxybutyric aciduria). *Am. J. Hum. Genet.* **63**, 399–408 (1998).
- Allen, P., Sommer, I. E., Jardri, R., Eysenck, M. W. & Hugdahl, K. Extrinsic and default mode networks in psychiatric conditions: Relationship to excitatory-inhibitory transmitter balance and early trauma. *Neurosci. Biobehav. Rev.* **99**, 90–100 (2019).
- Roestl, W. An historical perspective on GABAergic drugs. *Future Med. Chem.* **3**, 163–175 (2011).
- Spatazza, J., Mancia Leon, W. R. & Alvarez-Buylla, A. Transplantation of GABAergic interneurons for cell-based therapy. *Prog. Brain Res.* **231**, 57–85 (2017).
- Konya, Y., Bamba, T. & Fukusaki, E. Extra-facile chiral separation of amino acid enantiomers by LC-TOFMS analysis. *J. Biosci. Bioeng.* **121**, 349–353 (2016).
- Hollingsworth, E. B. *et al.* Biochemical characterization of a filtered synaptoneurosome preparation from guinea pig cerebral cortex: Cyclic adenosine 3':5'-monophosphate-generating systems, receptors, and enzymes. *J. Neurosci.* **5**, 2240–2253 (1985).
- Gajera, C. R. *et al.* Mass synaptometry: High-dimensional multi parametric assay for single synapses. *J. Neurosci. Methods* **312**, 73–83 (2019).
- Pamijlans, V., Krishnaswamy, P. R., Dumville, G. & Meister, A. Studies on the mechanism of glutamine synthesis; isolation and properties of the enzyme from sheep brain. *Biochemistry* **1**, 153–158 (1962).
- Kagan, H. M., Manning, L. R. & Meister, A. Stereospecific synthesis of alpha-methyl-L-glutamine by glutamine synthetase. *Biochemistry* **4**, 1063–1068 (1965).
- Gaisler-Salomon, I. *et al.* Glutaminase-deficient mice display hippocampal hypoactivity, insensitivity to pro-psychotic drugs and potentiated latent inhibition: Relevance to schizophrenia. *Neuropsychopharmacology* **34**, 2305–2322 (2009).
- Meister, A. [27] Glutamine synthetase from mammalian tissues. in *Methods in Enzymology*, Vol. 113, 185–199 (Academic Press, 1985).
- Kvamme, E., Torgner, I. A. A. & Svenneby, G. [30] Glutaminase from mammalian tissues. in *Methods in Enzymology*, Vol. 113, 241–256 (Academic Press, 1985).

20. Cluntun, A. A., Lukey, M. J., Cerione, R. A. & Locasale, J. W. Glutamine metabolism in cancer: Understanding the heterogeneity. *Trends Cancer Res.* **3**, 169–180 (2017).
21. Gross, M. I. *et al.* Antitumor activity of the glutaminase inhibitor CB-839 in triple-negative breast cancer. *Mol. Cancer Ther.* **13**, 890–901 (2014).
22. Yang, L. *et al.* Metabolic shifts toward glutamine regulate tumor growth, invasion and bioenergetics in ovarian cancer. *Mol. Syst. Biol.* **10**, 728 (2014).
23. Page, L. B. & Sidd, J. J. Medical management of primary hypertension. 2. *N. Engl. J. Med.* **287**, 1018–1023 (1972).
24. Black, D. G., Heagerty, A. M., Bing, R. F., Thurston, H. & Swales, J. D. Effects of treatment for hypertension on cerebral haemorrhage and infarction. *BMJ* **289**, 1145–1145 (1984).
25. Djurisic, M., Brott, B. K., Saw, N. L., Shamloo, M. & Shatz, C. J. Activity-dependent modulation of hippocampal synaptic plasticity via PirB and endocannabinoids. *Mol. Psychiatry* **24**, 1206–1219 (2019).
26. Rogers, D. C. *et al.* Behavioral and functional analysis of mouse phenotype: SHIRPA, a proposed protocol for comprehensive phenotype assessment. *Mamm. Genome* **8**, 711–713 (1997).
27. Bader, P. L. *et al.* Mouse model of Timothy syndrome recapitulates triad of autistic traits. *Proc. Natl. Acad. Sci. U.S.A.* **108**, 15432–15437 (2011).
28. Portmann, T. *et al.* Behavioral abnormalities and circuit defects in the basal ganglia of a mouse model of 16p11.2. Deletion syndrome. *Cell Rep.* **7**, 1077–1092 (2014).
29. Faizi, M. *et al.* Comprehensive behavioral phenotyping of Ts65Dn mouse model of Down Syndrome: Activation of β 1-adrenergic receptor by xamoterol as a potential cognitive enhancer. *Neurobiol. Dis.* **43**, 397–413 (2011).
30. Faizi, M. *et al.* Thy1-hAPP^{LonD/Swe+} mouse model of Alzheimer's disease displays broad behavioral deficits in sensorimotor, cognitive and social function. *Brain Behav.* **2**, 142–154 (2012).
31. Mah, G. T., Tejani, A. M. & Musini, V. M. Methyl dopa for primary hypertension. *Cochrane Database Syst. Rev.* **4**, CD003893 (2009).
32. Mzengeza, S., Venkatachalam, T. K. & Diksic, M. Asymmetric radiosynthesis of alpha-[¹¹C]methyl-L-tryptophan for PET studies. *Nucl. Med. Biol.* **22**, 303–307 (1995).
33. Chugani, H. T. *et al.* α -[¹¹C]-Methyl-L-tryptophan-PET in 191 patients with tuberous sclerosis complex. *Neurology* **81**, 674–680 (2013).
34. Gal, A. E., Avakian, S. & Martin, G. J. A Synthesis of DL- α -methylglutamic acid and some derivatives. *J. Am. Chem. Soc.* **76**, 4181–4182 (1954).
35. Takenishi, T. & Simamura, O. The syntheses from levulinic acid. A possible use of some 2-methyl-5-oxopyrrolidine-2-carboxylic esters as plasticizers. *BCSJ* **27**, 207–209 (1954).
36. Pfister, K. *et al.* α -Methyl- α -amino acids. I. Homologs of glutamic acid, methionine and diaminopimelic acid. *J. Am. Chem. Soc.* **77**, 697–700 (1955).
37. Fonda, M. L. Glutamate decarboxylase. Substrate specificity and inhibition by carboxylic acids. *Biochemistry* **11**, 1304–1309 (1972).
38. Fonda, M. L. & DeGrella, R. F. Inactivation of glutamate decarboxylase by bromopyruvate. *Biochem. Biophys. Res. Commun.* **56**, 451–458 (1974).
39. Grant, P. L., Basford, J. M. & John, R. A. An investigation of transient intermediates in the reaction of 2-methylglutamate with glutamate decarboxylase from *Escherichiacoli*. *Biochem. J* **241**, 699–704 (1987).
40. Gould, S. J., Guo, J., Geitmann, A. & Dejesus, K. Nucleoside intermediates in blasticidin S biosynthesis identified by the in vivo use of enzyme inhibitors. *Can. J. Chem.* **72**, 6–11 (1994).
41. Bolz, C. *et al.* Comparison of enzymatic properties and small molecule inhibition of γ -glutamyltranspeptidases from pathogenic and commensal bacteria. *Biol. Chem.* **398**, 341–357 (2017).
42. Haldeman, S., Huffman, R. D., Marshall, K. C. & McLennan, H. The antagonism of the glutamate-induced and synaptic excitations of thalamic neurones. *Brain Res.* **39**, 419–425 (1972).
43. Piggott, S. M., Kerkut, G. A. & Walker, R. J. Structure-activity studies on glutamate receptor sites of three identifiable neurones in the sub-oesophageal ganglia of *Helixaspersa*. *Comp. Biochem. Physiol. C* **51**, 91–100 (1975).
44. Shank, R. P. & Freeman, A. R. Agonistic and antagonistic activity of glutamate analogs on neuromuscular excitation in the walking limbs of lobsters. *J. Neurobiol.* **7**, 23–36 (1976).
45. Dudel, J. Aspartate and other inhibitors of excitatory synaptic transmission in crayfish muscle. *Pflugers Arch.* **369**, 7–16 (1977).
46. Bloomfield, S. A. & Dowling, J. E. Roles of aspartate and glutamate in synaptic transmission in rabbit retina I. Outer plexiform layer. *J. Neurophysiol.* **53**, 699–713 (1985).
47. Kern, H. L. & Ho, C.-K. Transport of dicarboxylic amino acids in the rat lens. *Ophthalmic Res.* **6**, 166–174 (1974).
48. Balcar, V. J., Schousboe, A., Spoerri, P. E. & Wolff, J. R. Differences between substrate specificities of L-glutamate uptake by neurons and glia, studied in cell lines and primary cultures. *Neurochem. Int.* **10**, 213–217 (1987).
49. Ganel, R. & Crosson, C. E. Modulation of human glutamate transporter activity by phorbol ester. *J. Neurochem.* **70**, 993–1000 (1998).
50. Miralles, A. & Olmos, G. [³H]kainic acid binding sites in chick cerebellar membranes. *Comp. Biochem. Physiol. C* **93**, 321–325 (1989).
51. Mori, M. & Shio, I. Glutamate transport and production in *Brevibacterium flavum*. *Agric. Biol. Chem.* **47**, 983–990 (1983).
52. Campbell, G. L., Bartel, R., Freidman, H. S. & Bigner, D. D. Effect of glutamate analogues on brain tumor cell lines. *J. Neurochem.* **45**, 1186–1192 (1985).
53. Roberts, P. J. & Anderson, S. D. Stimulatory effect of L-glutamate and related amino acids on [³H]dopamine release from rat striatum: An in vitro model for glutamate actions. *J. Neurochem.* **32**, 1539–1545 (1979).
54. Preuss, H. G. The effects of alpha-methylglutamate on ammonium excretion and renal ammonia production in rats. *Toxicol. Appl. Pharmacol.* **54**, 454–461 (1980).
55. Ichida, S. *et al.* Effects of neurotransmitter candidates on 45Ca uptake by cortical slices of rat brain: Stimulatory effect of L-glutamic acid. *Brain Res.* **248**, 305–311 (1982).
56. Kemp, M. C., Jane, D. E., Tse, H. W. & Roberts, P. J. Agonists of cyclic AMP-coupled metabotropic glutamate receptors in adult rat cortical slices. *Eur. J. Pharmacol.* **309**, 79–85 (1996).
57. Proceedings of the British Pharmacological Society. 10th–12th September, 1980. Abstracts. *Br. J. Pharmacol.* **72**, 487P–590P (1981).
58. Izumi, Y., Tatsumi, S., Imaida, M., Fukuda, Y. & Akabori, S. The preparation of optically active alpha-C-substituted glutamic acid. *Bull. Chem. Soc. Jpn.* **38**, 1338–1340 (1965).
59. Obrecht, D. *et al.* A novel synthesis of (R)- and (S)- α -alkylated aspartic and glutamic acids: α -alkylated aspartic succinimides as new type of β -turn type II and II' mimetics. *Tetrahedron* **51**, 10883–10900 (1995).
60. Islam, M. M. *et al.* Binding of C5-dicarboxylic substrate to aspartate aminotransferase: Implications for the conformational change at the transaldimination step. *Biochemistry* **44**, 8218–8229 (2005).
61. Colson, P. J. & Hegedus, L. S. Asymmetric synthesis of alpha-alkyl-alpha amino acids from chromium-carbene-complex-derived beta-lactams. *J. Org. Chem.* **58**, 5918–5924 (1993).
62. Tang, G., Tian, H. & Ma, D. Asymmetric Strecker reaction of γ -keto acids. Facile entry to α -substituted and α, γ -disubstituted glutamic acids. *Tetrahedron* **60**, 10547–10552 (2004).
63. Tsubogo, T., Kano, Y., Ikemoto, K., Yamashita, Y. & Kobayashi, S. Synthesis of optically active, unnatural α -substituted glutamic acid derivatives by a chiral calcium-catalyzed 1,4-addition reaction. *Tetrahedron Asymmetry* **21**, 1221–1225 (2010).

64. Bera, K., Satam, N. S. & Namboothiri, I. N. N. Enantioselective synthesis of quaternary α -amino acids via l-tert-leucine-derived squaramide-catalyzed conjugate addition of α -nitrocarboxylates to enones. *J. Org. Chem.* **81**, 5670–5680 (2016).
65. Holden, J. T., Utech, N. M. & Garth Reid, K. α -Methyl-L-glutamic acid uptake by high affinity dicarboxylic amino acid transport system in *Streptococcus faecalis*. *Biochim. Biophys. Acta Biomembr.* **394**, 55–64 (1975).
66. Vandenberg, R. J., Mitrovic, A. D., Chebib, M., Balcar, V. J. & Johnston, G. A. Contrasting modes of action of methylglutamate derivatives on the excitatory amino acid transporters, EAAT1 and EAAT2. *Mol. Pharmacol.* **51**, 809–815 (1997).
67. Yin, J. *et al.* Otud7a knockout mice recapitulate many neurological features of 15q13.3 microdeletion syndrome. *Am. J. Hum. Genet.* **102**, 296–308 (2018).
68. Min, S.-W. *et al.* Critical role of acetylation in tau-mediated neurodegeneration and cognitive deficits. *Nat. Med.* **21**, 1154–1162 (2015).
69. Evans, A. K. *et al.* Beta-adrenergic receptor antagonism is proinflammatory and exacerbates neuroinflammation in a mouse model of Alzheimer's disease. *Neurobiol. Dis.* **146**, 105089 (2020).

Acknowledgements

We wish to thank the Smart Foundation for a generous gift that supported this work. We thank Stanford ChEM-H Metabolomics Knowledge Center and Yuqin Dai for providing instrumentation and assistance with LC–MS/MS analyses. We thank Stanford University Mass Spectrometry facility and Karolina Krasinska for help with chiral LC–MS/MS analyses. We gratefully remember the kind mentorship of Professor Theodore Sourkes.

Author contributions

A.M.W. and T.J.M. conceived and supervised the study. A.M.W., S.A.B. and C.R.G. carried out the chemical and biochemical experiments. R.K.L. performed chemical characterization of pure materials. C.R.F. assisted with analytical method development. N.L.S. and M.S. planned, performed and supervised behavioral tests. A.M.W. and T.J.M. wrote the manuscript. All authors provided critical feedback and contributed to the final manuscript.

Competing interests

The authors declare no competing interests.

Additional information

Supplementary Information The online version contains supplementary material available at <https://doi.org/10.1038/s41598-021-87569-1>.

Correspondence and requests for materials should be addressed to T.J.M.

Reprints and permissions information is available at www.nature.com/reprints.

Publisher's note Springer Nature remains neutral with regard to jurisdictional claims in published maps and institutional affiliations.



Open Access This article is licensed under a Creative Commons Attribution 4.0 International License, which permits use, sharing, adaptation, distribution and reproduction in any medium or format, as long as you give appropriate credit to the original author(s) and the source, provide a link to the Creative Commons licence, and indicate if changes were made. The images or other third party material in this article are included in the article's Creative Commons licence, unless indicated otherwise in a credit line to the material. If material is not included in the article's Creative Commons licence and your intended use is not permitted by statutory regulation or exceeds the permitted use, you will need to obtain permission directly from the copyright holder. To view a copy of this licence, visit <http://creativecommons.org/licenses/by/4.0/>.

© The Author(s) 2021